

Research Article

Electrochemical Characterization of $\text{Li}_4\text{Ti}_5\text{O}_{12}/\text{C}$ Anode Material Prepared by Starch-Sol-Assisted Rheological Phase Method for Li-Ion Battery

Zhenpo Wang,¹ Guowei Xie,² and Lijun Gao^{2,3}

¹National Engineering Laboratory for Electric Vehicles, Beijing Institute of Technology, Beijing 100081, China

²Department of Chemistry, Nanchang University, Nanchang 330031, China

³School of Energy, Soochow University, Suzhou 215006, China

Correspondence should be addressed to Zhenpo Wang, wangzhenpo@bit.edu.cn and Lijun Gao, lijungao@yahoo.com

Received 7 January 2012; Revised 13 May 2012; Accepted 13 May 2012

Academic Editor: Arava Leela Mohana Reddy

Copyright © 2012 Zhenpo Wang et al. This is an open access article distributed under the Creative Commons Attribution License, which permits unrestricted use, distribution, and reproduction in any medium, provided the original work is properly cited.

$\text{Li}_4\text{Ti}_5\text{O}_{12}/\text{C}$ composite was synthesized by starch-sol-assisted rheological phase method using inexpensive raw material starch as carbon coating precursor. The $\text{Li}_4\text{Ti}_5\text{O}_{12}/\text{C}$ powder was characterized using XRD, SEM, and TG techniques. The synthesized $\text{Li}_4\text{Ti}_5\text{O}_{12}$ crystallites are cohesively covered by conductive carbon from starch sol which leads to increased conductivity, and the particle size of $\text{Li}_4\text{Ti}_5\text{O}_{12}/\text{C}$ is about 500 nm. The electrochemical performance of $\text{Li}_4\text{Ti}_5\text{O}_{12}/\text{C}$ was characterized by galvanostatic charge/discharge and EIS methods, and the results show that the $\text{Li}_4\text{Ti}_5\text{O}_{12}/\text{C}$ presents a high discharge capacity, high rate capability, and long cycle life. The capacity retention was at 87% (500 cycles at 1C) and 73.0% (2000 cycles at 20C) indicating promising high rate performance of $\text{Li}_4\text{Ti}_5\text{O}_{12}/\text{C}$ as anode material for lithium ion battery.

1. Introduction

Lithium ion batteries have been promising to be used in electric vehicle (EV) or hybrid electric vehicle (HEV). Currently, graphite was widely used as anode material for commercial Li-ion batteries in cell phones, laptops, and cameras [1]. However, its performance has not been satisfactory for applications in power systems which require frequent high rate charge/discharge such as in EV or HEV [2, 3]. Owing to the low lithium intercalation voltage of approximately 0.1 V (versus. Li/Li^+), lithium metal is easily deposited on the surface of graphite anode forming dendritic lithium particularly during fast charge, resulting in safety issue [2, 4]. Spinel $\text{Li}_4\text{Ti}_5\text{O}_{12}$ has acquired much attention as alternative anode to graphite in Li-ion batteries, due to its excellent reversibility, zero-strain structure, and high lithium ion mobility in the $\text{Li}_4\text{Ti}_5\text{O}_{12}$ lattice [5~7]. Especially, the material has a high Li-insertion voltage operating at 1.55 V (versus. Li/Li^+), which could hinder dendritic lithium formation [1, 5]. However, the low electronic conductivity

($10^{-13} \text{ S cm}^{-1}$) of $\text{Li}_4\text{Ti}_5\text{O}_{12}$ has been the main obstacle limiting rate performance of the material [6].

To improve electronic conductivity and electrochemical performance of $\text{Li}_4\text{Ti}_5\text{O}_{12}$, extensive works have been taken to address the issue, and the common strategies are to reduce particle size [4, 5], coat conductive material on the surface of $\text{Li}_4\text{Ti}_5\text{O}_{12}$ [2, 6, 7], or dope with other metal ions [8, 9]. Reducing particle size can shorten lithium ion diffusion distance and enhance both the electrode capability of Li storage and kinetics; thus the rate capability and electrochemical performance of electrode material can be improved [10]. Various metal ions such as Ni^{3+} , Ca^{3+} , Ta^{5+} , V^{5+} , and Mg^{2+} were employed in doping to substitute a small quantity of Li^+ or Ti^{4+} to improve the electronic conductivity and rate capability [8, 11–13]. Coating conductive materials on the surface of $\text{Li}_4\text{Ti}_5\text{O}_{12}$ can improve surface conductivity and reduce contact resistance [2]. Conductive materials (carbon black, carbon nanotubes, grapheme, Ag, Cu, and Sn [6, 10, 14, 15]) have been reported to be used to modify the electric conductivity of $\text{Li}_4\text{Ti}_5\text{O}_{12}$.

Many kinds of carbon have been examined as coating source in synthesis of $\text{Li}_4\text{Ti}_5\text{O}_{12}/\text{C}$ composite material with excellent electrochemical performance by conventional methods (e.g., solid state reaction and sol-gel methods) [3, 16, 17]. Starch is not only a good template in synthesis of various function materials with excellent electrochemical performance [18, 19] but also a good carbon source of coating to improve electric conductivity and reduce particle size [20]. Starch-sol-assisted rheological phase method has been developed to synthesize LiFePO_4/C composite [20]. However, to the best of our knowledge, synthesis of $\text{Li}_4\text{Ti}_5\text{O}_{12}/\text{C}$ composite has not been reported previously by using this method. In this work, we have used inexpensive starch as carbon source and adopted rheological phase method to prepare high-capacity $\text{Li}_4\text{Ti}_5\text{O}_{12}/\text{C}$ material. The composite was characterized by XRD, SEM, and TG techniques, and galvanostatic charge/discharge and EIS methods were used to examine electrochemical performance. The results show that carbon is cohesively coated on the surface of $\text{Li}_4\text{Ti}_5\text{O}_{12}$, and the composite has demonstrated high rate performance with good cycle stability when it was tested as anode in Li-ion batteries.

2. Experimental

2.1. Preparation of $\text{Li}_4\text{Ti}_5\text{O}_{12}$ and $\text{Li}_4\text{Ti}_5\text{O}_{12}/\text{C}$. The starting raw materials, TiO_2 -anatase (Aldrich), LiOH (Aldrich), and starch, were analytical grade and used without further purification. Firstly, the soluble starch (3.0 g starch/0.02 mol $\text{Li}_4\text{Ti}_5\text{O}_{12}$) was mixed with appropriate amount of deionized water; the resultant mixture was heated initially at 110°C until the solution became transparent under stirring in oil bath. Then the starch sol was mixed with stoichiometric amount of LiOH and TiO_2 (molar ratio of $\text{Ti}:\text{Li} = 4.2:5$) under vigorous agitation to obtain a solid-liquid rheological body, which appears to be a mushy slurry. Finally, the mushy slurry was transferred to tubular furnace and heated at the rate of $15^\circ\text{C min}^{-1}$ to 850°C and sintered at 850°C for 4 h in N_2 atmosphere and then cooled to room temperature to obtain a grey $\text{Li}_4\text{Ti}_5\text{O}_{12}/\text{C}$ powder. For comparison, pure $\text{Li}_4\text{Ti}_5\text{O}_{12}$ without carbon coating was synthesized by solid state method, which was prepared by mixing TiO_2 -anatase and LiOH (mole ratio of $\text{Li}:\text{Ti} = 4.2:5$); the mixture was heated at 850°C for 4 h in air to obtain well-crystallized white powder $\text{Li}_4\text{Ti}_5\text{O}_{12}$.

2.2. Electrode Fabrication. The electrochemical characterization was carried out by galvanostatic charge and discharge using a two-electrode type of 2025 coin cell. The working electrode was prepared with 84 wt.% active material $\text{Li}_4\text{Ti}_5\text{O}_{12}$ or $\text{Li}_4\text{Ti}_5\text{O}_{12}/\text{C}$, 10 wt.% super-P-Li carbon black, and 3 wt.% CMC (carboxymethyl cellulose sodium), and 3 wt.% SBR (styrene butadiene rubber) dissolved into deionized water to form mixed slurry. The slurries were dispersed in a planetary mixer and then spread uniformly on an aluminum foil by using doctor blade. Finally, the laminates were dried under vacuum at 100°C for 24 h before electrochemical evaluation. Electrode disks were punched

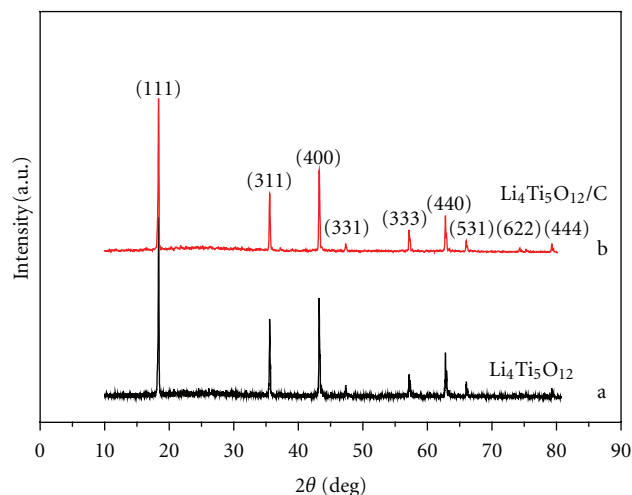


FIGURE 1: XRD pattern of pure spinel $\text{Li}_4\text{Ti}_5\text{O}_{12}$ (a) and $\text{Li}_4\text{Ti}_5\text{O}_{12}/\text{C}$ (b).

out of the laminates for the half-cell. The cells were assembled based on the configuration of $\text{Li}/\text{electrolyte}/\text{Li}_4\text{Ti}_5\text{O}_{12}/\text{C}$ (or $\text{Li}_4\text{Ti}_5\text{O}_{12}$) with a liquid electrolyte (1.3 M LiPF_6 in a mixture (1:3 by mass) of ethylene carbonate and dimethyl carbonate), metallic Li foil was used as the counter electrode in 2-electrode cell, and Celgard 2320 was used as the separator; the coin cells were assembled in a glove box (Braun, $[\text{O}_2] < 1 \text{ ppm}$, $[\text{H}_2\text{O}] < 1 \text{ ppm}$) filled with pure argon.

2.3. Characterization. The samples of $\text{Li}_4\text{Ti}_5\text{O}_{12}/\text{C}$ and $\text{Li}_4\text{Ti}_5\text{O}_{12}$ were characterized by X-ray diffraction (XRD) with D/Max-III A instrument using $\text{Cu K}\alpha$ ($\lambda = 1.54056 \text{ \AA}$) as radiation source at a scanning rate 2° min^{-1} for 2θ in the range of $10\text{--}80^\circ$ to identify the structure and phase. The morphologies of the samples were investigated by scanning electron microscopy (SEM, Hitachi S4800) and transmission electron microscopy (TEM, JEOL JEM-2010). Thermogravimetric and differential thermal analyses (TG/TGA) were performed on a TG/TGA instrument (Pyris Diamond) using a heating rate of $5^\circ\text{C}/\text{min}$.

The charge/discharge behavior and rate capacity of the cell were tested at various current densities in the range 1.0~2.0 V using land battery test station at room temperature. The AC impedance spectrum was employed at a constant potential of 1.55 V against Li metal electrode, the voltage amplitude of the AC signal was 5 mV, and the frequencies were scanned from 100 kHz to 100 mHz by using an electrochemical workstation IM6ex (Zahner).

3. Results and Discussion

3.1. Physicochemical Characterization. Figure 1 presents the XRD pattern of the two samples. Figure 1(a) is for the pure $\text{Li}_4\text{Ti}_5\text{O}_{12}$ prepared by solid-state method, and Figure 1(b) is for the $\text{Li}_4\text{Ti}_5\text{O}_{12}/\text{C}$ composite synthesized by starch-sol-assisted rheological phase method. According to JCPDS file

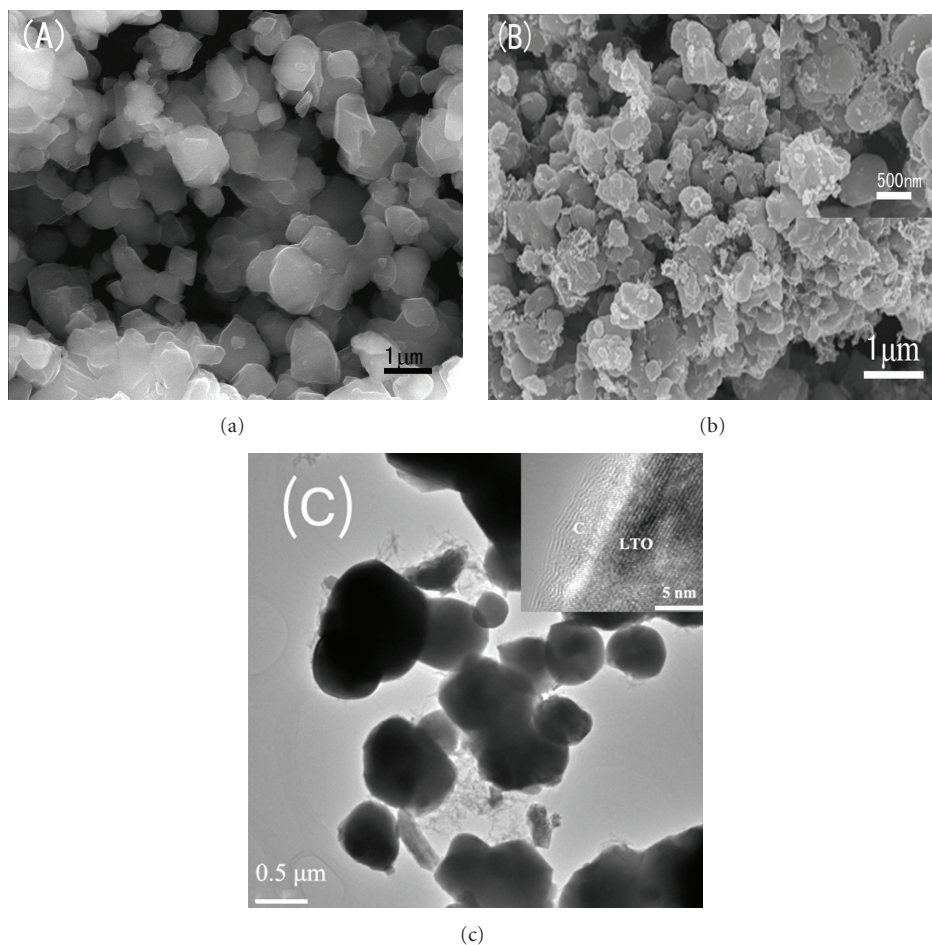


FIGURE 2: SEM images of pure $\text{Li}_4\text{Ti}_5\text{O}_{12}$ (a) and $\text{Li}_4\text{Ti}_5\text{O}_{12}/\text{C}$ composite (b). HRTEM image and the inset (c) clearly show the carbon coating on the $\text{Li}_4\text{Ti}_5\text{O}_{12}$ crystallites.

no. 49-0207, all the main peaks are investigated, which correspond to $\text{Li}_4\text{Ti}_5\text{O}_{12}$ without other impurity phases. The pattern could be indexed to spinel structure with $\text{Fd}3\text{m}$ space group. The lattice parameter of “a” for $\text{Li}_4\text{Ti}_5\text{O}_{12}/\text{C}$ composite is 8.359 Å, which is close to the reported value of the literature [21]. No carbon diffraction peak is observed in Figure 1(b) since the carbon generated from starch is in low content, and it is amorphous, which suggests that the addition of starch in the precursor does not influence the formation of spinel $\text{Li}_4\text{Ti}_5\text{O}_{12}$ crystal during heat treatment in the N_2 atmosphere. It was found through Scherrer equation that the average crystallite size was about 400~600 nm.

For comparison, Figure 2(a) shows the SEM image of pure $\text{Li}_4\text{Ti}_5\text{O}_{12}$ synthesized by solid-state method. The $\text{Li}_4\text{Ti}_5\text{O}_{12}$ crystallites have smooth sphere-like shape morphology, large blocks of particles at about 700 nm~1 μm in size. Figure 2(b) presents SEM image of the $\text{Li}_4\text{Ti}_5\text{O}_{12}/\text{C}$ composite. It is seen that the carbon uniformly covers the surface of $\text{Li}_4\text{Ti}_5\text{O}_{12}$ and links together forming a carbon network. The particles of $\text{Li}_4\text{Ti}_5\text{O}_{12}/\text{C}$ have a relatively less extent of agglomeration, and the average particle size is about 500 nm, which is consistent with the result from

XRD calculation. Figure 2(c) shows the high-resolution TEM image of the $\text{Li}_4\text{Ti}_5\text{O}_{12}/\text{C}$ composite; it is clearly seen that the $\text{Li}_4\text{Ti}_5\text{O}_{12}$ has sphere-like shape and the particle size ranges from 400 nm to 600 nm, consistent with the SEM observation in Figure 2(b). The inset HRTEM also shows a 5 nm thick carbon film coated on the surface of $\text{Li}_4\text{Ti}_5\text{O}_{12}$ crystallites. Due to the adhesive nature of starch sol, the carbon binds cohesively on the surface of reactants during calcination process, and the heating process further results in decomposition of the starch into a carbonaceous deposit on the surface of $\text{Li}_4\text{Ti}_5\text{O}_{12}$. The carbonization of starch precursor effectively restrains the growth of $\text{Li}_4\text{Ti}_5\text{O}_{12}$ crystallites into larger size.

In order to investigate the content of carbon in the composite $\text{Li}_4\text{Ti}_5\text{O}_{12}/\text{C}$, TG/DTA was carried out with $15^\circ\text{C min}^{-1}$ heating rate from 30°C to 1000°C in air. The profile of TG/DTA is given in Figure 3. A broad exothermic peak appears at about 580°C, which is owing to the combustion of the starch into carbonaceous species on the surface of $\text{Li}_4\text{Ti}_5\text{O}_{12}$, and the TG indicates that the content of carbon in the composite $\text{Li}_4\text{Ti}_5\text{O}_{12}/\text{C}$ is about 5%. The weight loss after 700°C is due to the loss of lithium during the high temperature process [22, 23].

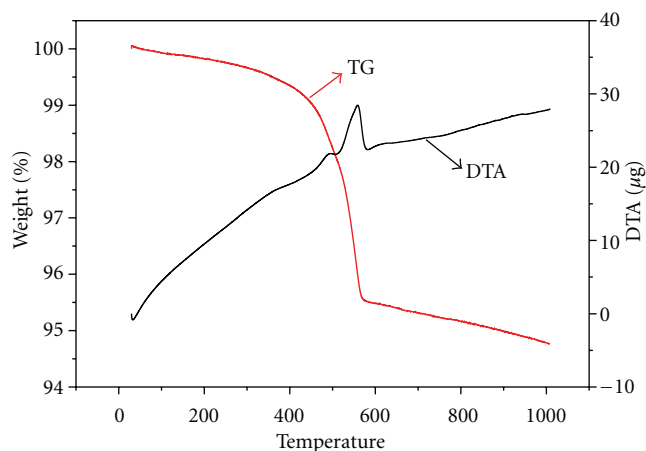


FIGURE 3: TG/TGA profile of $\text{Li}_4\text{Ti}_5\text{O}_{12}/\text{C}$ measured in air atmosphere.

3.2. Electrochemical Characterization. The electrochemical performance of $\text{Li}_4\text{Ti}_5\text{O}_{12}/\text{C}$ and $\text{Li}_4\text{Ti}_5\text{O}_{12}$ electrodes was examined in coin cells with metallic lithium as counter electrode. The cycle behavior of the cell was investigated in the range of 1.0~2.0V. The initial charge-discharge curves of $\text{Li}_4\text{Ti}_5\text{O}_{12}$ (a) and $\text{Li}_4\text{Ti}_5\text{O}_{12}/\text{C}$ (b) at various charge/discharge rates are compared as shown in Figure 4. At the current density of 0.2C, the initial discharge capacity of $\text{Li}_4\text{Ti}_5\text{O}_{12}/\text{C}$ is 171.5 mAh g^{-1} , which is very close to its theoretical capacity (175 mAh g^{-1}), and at a 20C high rate, the capacity is 110 mAh g^{-1} . Furthermore, the profile shows very flat discharge/discharge plateau at around 1.55 V (versus. Li/Li^+). However, the initial specific capacity of pure $\text{Li}_4\text{Ti}_5\text{O}_{12}$ is only about 160 mAh g^{-1} at 0.2C and 34.5 mAh g^{-1} at 20C, the cell voltage is lower, and the polarization increases with the increasing of charge/discharge rate, as it is shown that the plateau voltage difference between charge and discharge is 60 mV at 0.5C and 440 mV at 20C. With carbon-coated $\text{Li}_4\text{Ti}_5\text{O}_{12}/\text{C}$, the polarization was obviously smaller as it is seen that the voltage gap between charge and discharge plateau is narrower as shown in Figure 4(b), and the plateau appears more flat especially at high rates. This improved high-rate discharge ability of $\text{Li}_4\text{Ti}_5\text{O}_{12}/\text{C}$ which may be attributed to the facts that (1) the carbon generated from starch was coated uniformly on the surface of $\text{Li}_4\text{Ti}_5\text{O}_{12}$ resulting in enhanced electrical conductivity and (2) the starch limited the growth of $\text{Li}_4\text{Ti}_5\text{O}_{12}$ crystallite size during calcination process, which benefits Li^+ diffusion with shortened distance in $\text{Li}_4\text{Ti}_5\text{O}_{12}$.

To investigate the rate capability, the $\text{Li}_4\text{Ti}_5\text{O}_{12}$ and $\text{Li}_4\text{Ti}_5\text{O}_{12}/\text{C}$ have been cycled at various rates from 0.2C to 20C, and the results are presented in Figure 5. The charge and discharge cycles were taken for 5 cycles at each rate. As shown in Figure 5(a), the specific discharge capacity is gradually decreased with increased rates. However, the degree of capacity decay of $\text{Li}_4\text{Ti}_5\text{O}_{12}/\text{C}$ sample is in less extent in comparison with the pure $\text{Li}_4\text{Ti}_5\text{O}_{12}$. At 20C the capacity remains 75% of that at 0.2C for $\text{Li}_4\text{Ti}_5\text{O}_{12}/\text{C}$, but for pure $\text{Li}_4\text{Ti}_5\text{O}_{12}$ the capacity is about 24% between 20C

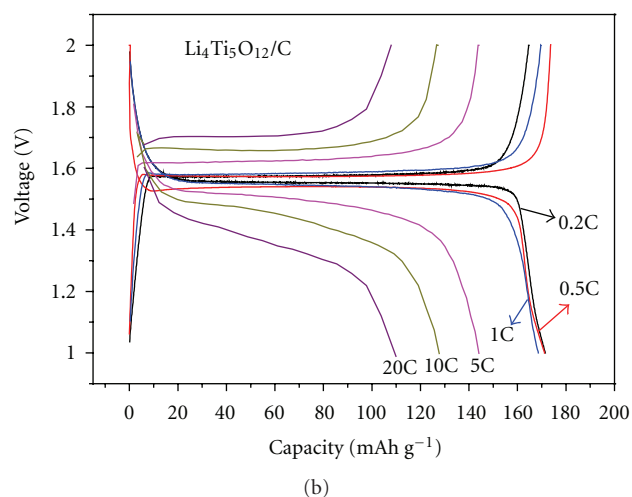
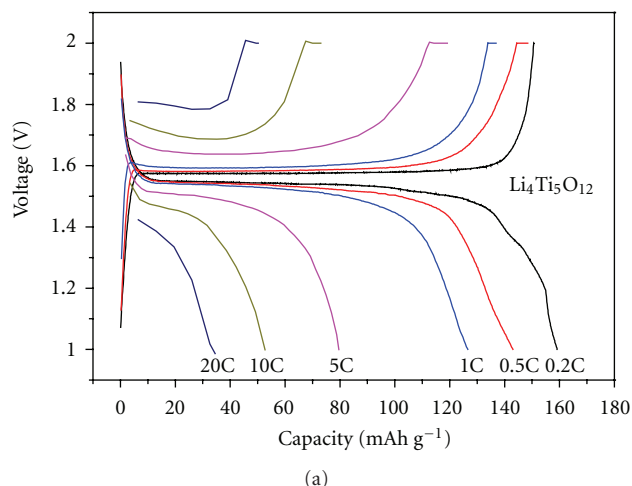


FIGURE 4: The initial charge/discharge profiles of spinel $\text{Li}_4\text{Ti}_5\text{O}_{12}$ (a) and $\text{Li}_4\text{Ti}_5\text{O}_{12}/\text{C}$ (b) at various rates from 0.2C to 20C.

and 0.2C rates. Figure 5(b) shows the cycle performance of the $\text{Li}_4\text{Ti}_5\text{O}_{12}/\text{C}$ electrode at 1C and 20C. The initial specific discharge capacity of $\text{Li}_4\text{Ti}_5\text{O}_{12}/\text{C}$ is 168.6 mAh g^{-1} at 1C, and it retains 87% after 500 cycles. At 20C cycle rate, the sample exhibits an initial discharge capacity of 110 mAh g^{-1} in Figure 5(b), and there is no apparent capacity fading in the 1st~1000th cycles at 20C, indicating excellent rate performance of the material. After 2000 cycles, the capacity remains 73% of initial value. Compared to the literature data, the performance of the $\text{Li}_4\text{Ti}_5\text{O}_{12}$ and $\text{Li}_4\text{Ti}_5\text{O}_{12}/\text{C}$ composites synthesized by starch-sol-assisted rheological phase method in this work is superior to those reported in [4, 6, 24–28]. This cycle performance can be ascribed to the fact that the $\text{Li}_4\text{Ti}_5\text{O}_{12}$ itself has a low volume expansion structure, and the cohesive carbon coating that resulted from the starch sol rheological phase method increased electrical conductivity in $\text{Li}_4\text{Ti}_5\text{O}_{12}/\text{C}$.

EIS technique has been considered as an effective way to identify diffusion phenomena in electronic and ionic conductors. To study conductivities of the $\text{Li}_4\text{Ti}_5\text{O}_{12}/\text{C}$ and $\text{Li}_4\text{Ti}_5\text{O}_{12}$, EIS measurements were carried out at 1.55 V at

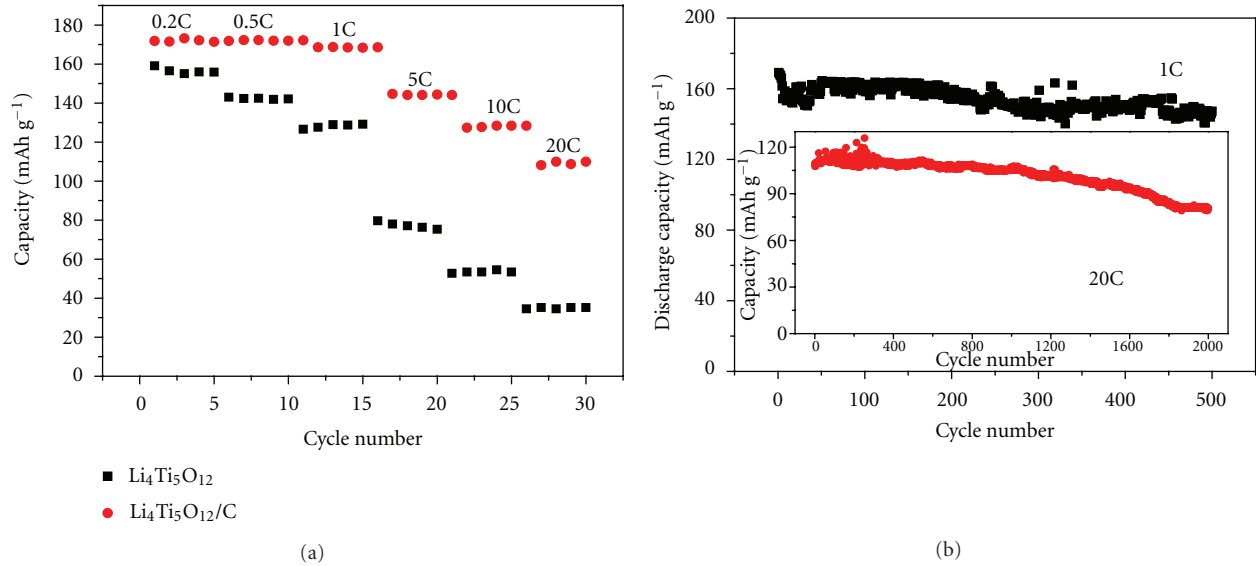


FIGURE 5: Comparison of rate capability of pure Li₄Ti₅O₁₂ and Li₄Ti₅O₁₂/C at various rates (a). Cycle performance of the Li₄Ti₅O₁₂/C electrode at 1C and 20C rates (b).

room temperature. The Nyquist plots of Li₄Ti₅O₁₂/C and Li₄Ti₅O₁₂ electrodes as well as the fitting results using an equivalent circuit are given in Figure 6. Both Nyquist plots are composed of a depressed semicircle in high frequency and a straight line in low frequency region in Figure 6(a). The solution resistance R_s of the cell from Z' axis interception at high frequency includes both electrolyte and electrode contact resistance. The charge transfer resistance R_{ct} is determined by the semicircle in the middle frequency range, which is mainly related to the electrochemical reaction at the electrolyte/electrode interface. The straight line in low frequency range is attributed to the Warburg impedance Z_w , which is due to the solid-state diffusion of Li⁺ ions into the bulk of active material. It can be seen from Figure 6(a) that the Li₄Ti₅O₁₂/C electrode displayed a much lower impedance than that of pure Li₄Ti₅O₁₂ which is similarly observed in [16, 29].

The equivalent circuit model is depicted in Figure 6(b), where the R_s and R_{ct} are solution resistance and charge transfer resistance, respectively. CPE is the constant phase-angle element, involving double layer capacitance of the electrolyte-electrode interface. R_f is the surface polarization resistance, and the C_f is the surface capacitance. The equivalent circuit model is well suited to the fitting of experiment data, and the simulation results of the EIS data for the Li₄Ti₅O₁₂/C and Li₄Ti₅O₁₂ electrodes are given in Table 1. It can be seen that the R_s and R_{ct} are much smaller for the Li₄Ti₅O₁₂/C electrode ($R_s = 1.92 \Omega$, $R_{ct} = 24 \Omega$) than for the pure Li₄Ti₅O₁₂ ($R_s = 3.33 \Omega$, $R_{ct} = 107 \Omega$). This result indicates that the carbon coating has enabled easier charge transfer at electrode/electrolyte interface, and the overall battery internal resistance is also decreased. The electrode polarization resistance of Li₄Ti₅O₁₂/C ($R_f = 0.184 \Omega$) is much smaller than that of Li₄Ti₅O₁₂ ($R_f = 1.08 \Omega$), which implies that the carbon reduced the polarization. The results

are also consistent with the charge/discharge curves shown in Figure 4. The two values of Z_w are almost identical; this is reasonable since the Li⁺ diffusion rate in Li₄Ti₅O₁₂ crystal lattice should be independent of carbon coating. The *in situ* starch sol coating in the synthesis of Li₄Ti₅O₁₂ significantly enhances the conductivity of Li₄Ti₅O₁₂ material. The adhesive conductive carbon coating facilitates electronic conductive paths in the Li₄Ti₅O₁₂ particle surroundings, that is considered a key factor in improving the discharge capacity, rate capability, and cycle life of the Li₄Ti₅O₁₂/C material.

4. Conclusions

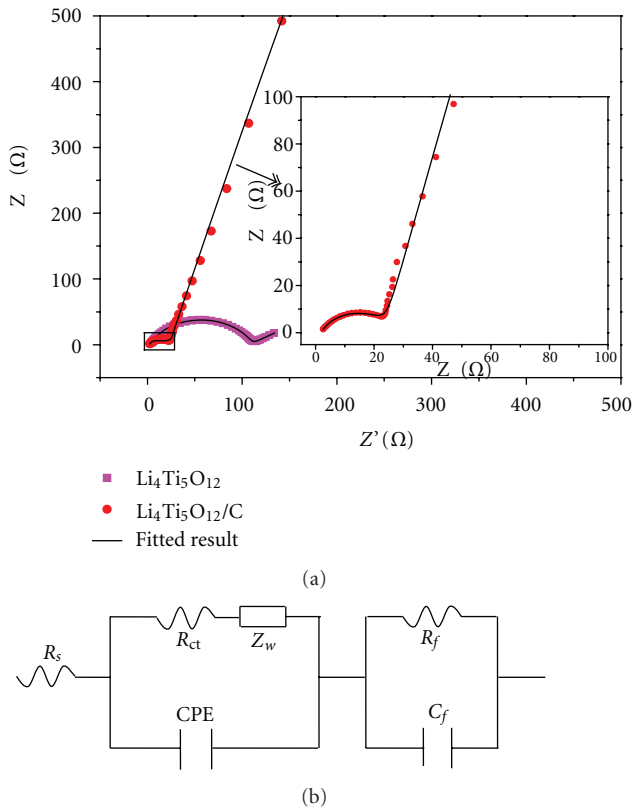
With the starch precursor as carbon source, the carbon was cohesively coated on the surface of Li₄Ti₅O₁₂ crystallites in the Li₄Ti₅O₁₂/C composite by using starch-sol-assisted rheological phase method. This synthesis approach is relatively simple and effective to obtain the high electronic conductive material. The electrochemical characterization indicates that the Li₄Ti₅O₁₂/C exhibits high rate capability and long cycle life compared to pure Li₄Ti₅O₁₂ from solid-state method. The Li₄Ti₅O₁₂/C anode shows specific capacity of 168.6 mAh g⁻¹ at 1C and 110 mAh g⁻¹ at 20C, and the discharge capacity retains 73% after 2000 cycles at 20C cycle rate. The excellent rate capability and cycling performance of Li₄Ti₅O₁₂/C are mainly attributed to the cohesive carbon coating that enhances conductivity and to the intrinsic structural stability of Li₄Ti₅O₁₂ that allows reversible Li⁺ intercalation in charge-discharge process.

Acknowledgments

The authors are grateful for funding support from the Natural Science Foundation of China (project no. 61004092).

TABLE 1: EIS simulation parameters of $\text{Li}_4\text{Ti}_5\text{O}_{12}$ and $\text{Li}_4\text{Ti}_5\text{O}_{12}/\text{C}$ from the equivalent circuit.

Sample	R_s ($\Omega \text{ cm}^2$)	R_{ct} ($\Omega \text{ cm}^2$)	CPE ($\text{S}^n \text{ cm}^{-2}$)	W ($\text{S}^{0.5} \text{ cm}^{-2}$)	R_f ($\Omega \text{ cm}^2$)	C_f ($\text{S}^n \text{ cm}^{-2}$)
$\text{Li}_4\text{Ti}_5\text{O}_{12}$	3.33	107	2.5×10^{-4}	2.55×10^{-4}	1.08	8.66×10^{-6}
$\text{Li}_4\text{Ti}_5\text{O}_{12}/\text{C}$	1.92	24	2.45×10^{-4}	2.2×10^{-4}	0.184	2.72×10^{-6}

FIGURE 6: EIS Nyquist plots of the $\text{Li}_4\text{Ti}_5\text{O}_{12}$ and $\text{Li}_4\text{Ti}_5\text{O}_{12}/\text{C}$ electrode (a) and the corresponding equivalent circuit model that is used to fit the experimental data (b).

References

- [1] L. Yuan, R. Cai, P. Gu, and Z. Shao, "Synthesis of lithium insertion material $\text{Li}_4\text{Ti}_5\text{O}_{12}$ from rutile TiO_2 via surface activation," *Journal of Power Sources*, vol. 195, no. 9, pp. 2883–2887, 2010.
- [2] L. Zhao, Y.-S. Hu, H. Li, Z. Wang, and L. Chen, "Porous $\text{Li}_4\text{Ti}_5\text{O}_{12}$ coated with N-doped carbon from ionic liquids for Li-ion batteries," *Advanced Materials*, vol. 23, no. 11, pp. 1385–1388, 2011.
- [3] M. M. Rahman, J.-Z. Wang, M. F. Hassan, D. Wexler, and H. K. Liu, "Amorphous carbon coated high grain boundary density dual phase $\text{Li}_4\text{Ti}_5\text{O}_{12}$ - TiO_2 : a nanocomposite anode material for Li-ion batteries," *Advanced Energy Materials*, vol. 1, no. 2, pp. 212–220, 2011.
- [4] Y. Wang, H. Liu, K. Wang, H. Eiji, Y. Wang, and H. Zhou, "Synthesis and electrochemical performance of nano-sized $\text{Li}_4\text{Ti}_5\text{O}_{12}$ with double surface modification of Ti(III) and carbon," *Journal of Materials Chemistry*, vol. 19, no. 37, p. 6789, 2009.
- [5] K. Amine, I. Belharouak, Z. Chen et al., "Nanostructured anode material for high-power battery system in electric vehicles," *Advanced Materials*, vol. 22, no. 28, pp. 3052–3057, 2010.
- [6] L. Shen, C. Yuan, H. Luo, X. Zhang, K. Xu, and F. Zhang, "In situ growth of $\text{Li}_4\text{Ti}_5\text{O}_{12}$ on multi-walled carbon nanotubes: novel coaxial nanocables for high rate lithium ion batteries," *Journal of Materials Chemistry*, vol. 21, no. 3, pp. 761–767, 2011.
- [7] K.-S. Park, A. Benayad, D. J. Kang, and S. G. Doo, "Nitridation-driven conductive $\text{Li}_4\text{Ti}_5\text{O}_{12}$ for lithium ion batteries," *Journal of the American Chemical Society*, vol. 130, no. 45, pp. 14930–14931, 2008.
- [8] J. Wolfenstine and J. L. Allen, "Electrical conductivity and charge compensation in Ta doped $\text{Li}_4\text{Ti}_5\text{O}_{12}$," *Journal of Power Sources*, vol. 180, no. 1, pp. 582–585, 2008.
- [9] S. Huang, Z. Wen, X. Zhu, and Z. Lin, "Effects of dopant on the electrochemical performance of $\text{Li}_4\text{Ti}_5\text{O}_{12}$ as electrode material for lithium ion batteries," *Journal of Power Sources*, vol. 165, no. 1, pp. 408–412, 2007.
- [10] L. Cheng, J. Yan, G.-N. Zhu, J.-Y. Luo, C.-X. Wang, and Y.-Y. Xia, "General synthesis of carbon-coated nanostructure $\text{Li}_4\text{Ti}_5\text{O}_{12}$ as a high rate electrode material for Li-ion intercalation," *Journal of Materials Chemistry*, vol. 20, no. 3, pp. 595–602, 2010.
- [11] A. D. Robertson, L. Trevino, H. Tukamoto, and J. T. S. Irvine, "New inorganic spinel oxides for use as negative electrode materials in future lithium-ion batteries," *Journal of Power Sources*, vol. 81-82, pp. 352–357, 1999.
- [12] S. Shi, C. Ouyang, M. Lei, and W. Tang, "Effect of Mg-doping on the structural and electronic properties of LiCoO_2 : a first-principles investigation," *Journal of Power Sources*, vol. 171, no. 2, pp. 908–912, 2007.
- [13] P. Kubiak, A. Garcia, M. Womes et al., "Phase transition in the spinel $\text{Li}_4\text{Ti}_5\text{O}_{12}$ induced by lithium insertion-influence of the substitutions Ti/V, Ti/Mn, Ti/Fe," *Journal of Power Sources*, vol. 119–121, pp. 626–630, 2003.
- [14] S. Huang, Z. Wen, B. Lin, J. Han, and X. Xu, "The high-rate performance of the newly designed $\text{Li}_4\text{Ti}_5\text{O}_{12}/\text{Cu}$ composite anode for lithium ion batteries," *Journal of Alloys and Compounds*, vol. 457, no. 1-2, pp. 400–403, 2008.
- [15] A. Sivashanmugam, S. Gopukumar, R. Thirunakaran, C. Nithya, and S. Prema, "Novel $\text{Li}_4\text{Ti}_5\text{O}_{12}/\text{Sn}$ nano-composites as anode material for lithium ion batteries," *Materials Research Bulletin*, vol. 46, no. 4, pp. 492–500, 2011.
- [16] T. Yuan, X. Yu, R. Cai, Y. Zhou, and Z. Shao, "Synthesis of pristine and carbon-coated $\text{Li}_4\text{Ti}_5\text{O}_{12}$ and their low-temperature electrochemical performance," *Journal of Power Sources*, vol. 195, no. 15, pp. 4997–5004, 2010.
- [17] H.-G. Jung, J. Kim, B. Scrosati, and Y. K. Sun, "Micron-sized, carbon-coated $\text{Li}_4\text{Ti}_5\text{O}_{12}$ as high power anode material for

- advanced lithium batteries,” *Journal of Power Sources*, vol. 196, no. 18, pp. 7763–7766, 2011.
- [18] W. Tang, S. Tian, L. L. Liu et al., “Nanochain LiMn_2O_4 as ultra-fast cathode material for aqueous rechargeable lithium batteries,” *Electrochemistry Communications*, vol. 13, no. 2, pp. 205–208, 2011.
- [19] V. Singh, S. K. Singh, S. Pandey, and P. Kumar, “Sol-gel synthesis and characterization of adsorbent and photoluminescent nanocomposites of starch and silica,” *Journal of Non-Crystalline Solids*, vol. 357, no. 1, pp. 194–201, 2011.
- [20] Y. Huang, H. Ren, S. Yin, Y. Wang, Z. Peng, and Y. Zhou, “Synthesis of LiFePO_4/C composite with high-rate performance by starch sol assisted rheological phase method,” *Journal of Power Sources*, vol. 195, no. 2, pp. 610–613, 2010.
- [21] S. C. Lee, S. M. Lee, J. W. Lee et al., “Spinel $\text{Li}_4\text{Ti}_5\text{O}_{12}$ nanotubes for energy storage materials,” *Journal of Physical Chemistry C*, vol. 113, no. 42, pp. 18420–18423, 2009.
- [22] M. Hirayama, K. Kim, T. Tadjigamori, W. Cho, and R. Kanno, “Epitaxial growth and electrochemical properties of $\text{Li}_4\text{Ti}_5\text{O}_{12}$ thin-film lithium battery anodes,” *Dalton Transactions*, vol. 40, no. 12, pp. 2882–2887, 2011.
- [23] L. Kavan, J. Prochazka, T. M. Spittler et al., “Li insertion into $\text{Li}_4\text{Ti}_5\text{O}_{12}$ (Spinel),” *Journal of The Electrochemical Society*, vol. 150, no. 7, pp. A1000–A1007, 2003.
- [24] L. Shen, C. Yuan, H. Luo, X. Zhang, K. Xu, and Y. Xia, “Facile synthesis of hierarchically porous $\text{Li}_4\text{Ti}_5\text{O}_{12}$ microspheres for high rate lithium ion batteries,” *Journal of Materials Chemistry*, vol. 20, no. 33, pp. 6998–7004, 2010.
- [25] G. Xie, J. Ni, X. Liao, and L. Gao, “Filter paper templated synthesis of chain-structured $\text{Li}_4\text{Ti}_5\text{O}_{12}/\text{C}$ composite for Li-ion batteries,” *Materials Letters*, vol. 78, pp. 177–179, 2012.
- [26] G. F. Yan, H. Fang, H. Zhao, G. Li, Y. Yang, and L. Li, “Ball milling-assisted sol-gel route to $\text{Li}_4\text{Ti}_5\text{O}_{12}$ and its electrochemical properties,” *Journal of Alloys and Compounds*, vol. 470, no. 1–2, pp. 544–547, 2009.
- [27] J. Gao, C. Jiang, J. Ying, and C. Wan, “Preparation and characterization of high-density spherical $\text{Li}_4\text{Ti}_5\text{O}_{12}$ anode material for lithium secondary batteries,” *Journal of Power Sources*, vol. 155, no. 2, pp. 364–367, 2006.
- [28] Y. Qiao, X. Luo, Y. Liu, and Y. Huang, “ $\text{Li}_4\text{Ti}_5\text{O}_{12}$ nanocrystallites for high-rate lithium-ion batteries synthesized by a rapid microwave-assisted solid-state process,” *Electrochimica Acta*, vol. 63, no. 29, pp. 118–123, 2012.
- [29] L. Yang and J. Gao, “ $\text{Li}_4\text{Ti}_5\text{O}_{12}/\text{C}$ composite electrode material synthesized involving conductive carbon precursor for Li-ion battery,” *Journal of Alloys and Compounds*, vol. 485, no. 1–2, pp. 427–434, 2009.



Hindawi

Submit your manuscripts at
<http://www.hindawi.com>

